Strongly Correlated Photon Transport in Waveguide Quantum Electrodynamics with Weakly Coupled Emitters

Mahmoodian, Sahand; epulkovskis, Mantas; Das, Sumanta Kumar; Lodahl, Peter; Hammerer, Klemens; Sørensen, Anders Søndberg

Published in:
Physical Review Letters

DOI:
10.1103/PhysRevLett.121.143601

Publication date:
2018

Document version
Publisher's PDF, also known as Version of record

Strongly Correlated Photon Transport in Waveguide Quantum Electrodynamics with Weakly Coupled Emitters

Sahand Mahmoodian,[1,2,*] Mantas Čepulkovskis,[3] Sumanta Das,[3] Peter Lodahl,[3] Klemens Hammerer,[1] and Anders S. Sørensen[3]

[1]Institute for Theoretical Physics, Institute for Gravitational Physics (Albert Einstein Institute), Leibniz University Hannover, Appelstraße 2, 30167 Hannover, Germany

[2]Niels Bohr Institute, University of Copenhagen, Blegdamsvej 17, DK-2100 Copenhagen, Denmark

[3]Center for Hybrid Quantum Networks (Hy-Q), Niels Bohr Institute, University of Copenhagen, Blegdamsvej 17, DK-2100 Copenhagen, Denmark

(Received 9 March 2018; published 3 October 2018)

We show that strongly correlated photon transport can be observed in waveguides containing optically dense ensembles of emitters. Remarkably, this occurs even for weak coupling efficiencies. Specifically, we compute the photon transport properties through a chirally coupled system of N two-level systems driven by a weak coherent field, where each emitter can also scatter photons out of the waveguide. The photon correlations arise due to an interplay of nonlinearity and coupling to a loss reservoir, which creates a strong effective interaction between transmitted photons. The highly correlated photon states are less susceptible to losses than uncorrelated photons and have a power-law decay with N. This is described using a simple universal asymptotic solution governed by a single scaling parameter which describes photon bunching and power transmission. We show numerically that, for randomly placed emitters, these results hold even in systems without chirality. The effect can be observed in existing tapered fiber setups with trapped atoms.

DOI: 10.1103/PhysRevLett.121.143601

Describing the dynamics of quantum systems that are far from equilibrium is currently one of the main challenges of physics. Considerable effort is put into understanding these systems, e.g., in quantum many-body physics and nonlinear dynamics [1,2], as well as developing quantum simulators to investigate them [3]. In the field of mesoscopic physics such dynamics are especially studied through quantum transport [4–6]. Recently, quantum transport of photons has emerged as an analogous system to study nonequilibrium quantum dynamics in optical systems [7–9]. Most notably this has been investigated in weakly driven strongly interacting Rydberg gases, where effective photon-photon interactions at the few-photon level have been observed [10–15]. This has led to the demonstration of fascinating new phenomena such as correlated two- [16,17] and three-photon [18–20] bound states. Similar photon-photon interactions are also investigated for quantum emitters strongly coupled to optical waveguides or cavities. Here the intrinsic nonlinearity of a single emitter plays the role of a nonlinear medium [21–23]. Significant effort has therefore been put into creating light-matter interfaces between an emitter and a single optical mode with near-unity coupling efficiency $\beta \sim 1$ so that dissipation is minimized [24,25]. Contrary to this, we consider quantum transport through a strongly dissipative system consisting of $N \gg 1$ quantum emitters coupled to a waveguide. We analytically compute the dynamics of this system in the case of chiral coupling [26–36], where emitters only couple to photons propagating to the right [Fig. 1(a)]. Surprisingly, we find that the interplay of weak nonlinearity and strong dissipation leads to the emergence of highly nonlinear transmission and strongly correlated photon states at the output. Previously, such dissipatively induced photon correlations have been studied for strong optical nonlinearities [12,37,38]. Since these dynamics can occur even for weakly coupled emitters $\beta \ll 1$, they are readily observable in a larger range of

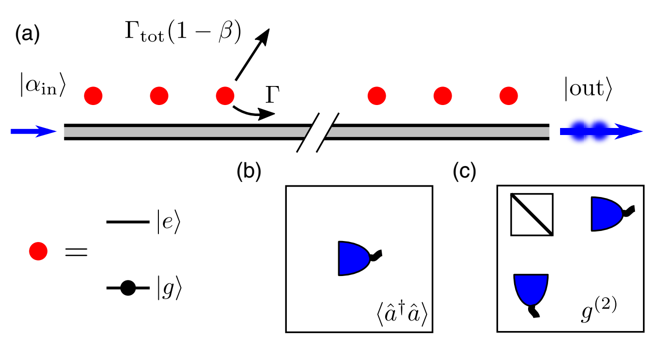

FIG. 1. (a) N chirally coupled two-level emitters (red circles) driven by an external coherent field $|\alpha_{\rm in}\rangle$ with a corresponding strongly correlated output photon state $|{\rm out}\rangle$. Each emitter is coupled to the waveguide with a decay rate $\Gamma = \beta\Gamma_{\rm tot}$ and to external loss modes with a decay rate $\Gamma_{\rm tot}(1-\beta)$. The output state is probed by measuring (b) power $\langle \hat{a}^\dagger \hat{a} \rangle$ or (c) the normalized second-order correlation function $g^{(2)}$.

systems, e.g., in experiments on atoms coupled to nanofibers [27,39–42].

The phenomena we investigate are based on dissipation and can thus only be observed in optically dense ensembles. Specifically, when two resonant photons interact with the same atom, they can exchange energy, creating correlated red- and blue-detuned photons (sidebands). Since losses are strongest on resonance, resonant uncorrelated photons suffer strong loss (exponential scaling with N), while off-resonant correlated photons incur reduced loss. The smallest detunings are lost first, so that the decay rate constantly decreases with subsequent atoms since the remaining photons have larger detunings. This leads to a power-law decay of the transmission and the output being dominated by strongly correlated (bunched) photons. Such power-law decay is ubiquitous in critical [43] or chaotic [44] systems and is linked to scale invariance and the absence of a characteristic length scale, so that the microscopic details of the system become irrelevant. Analogously, we find that in the limit of large optical depth, the dynamics attains a universal scaling relation, which becomes independent of the precise value of the coupling efficiency. In the following we derive these results analytically, assuming chiral interactions, but we show numerically that these conclusions are robust and also apply to bidirectional interactions, i.e., nonchiral, for weakly coupled randomly placed emitters.

We consider a system of N-chirally coupled two-level emitters continuously driven by a weak coherent field while dissipatively coupled to a loss reservoir [Fig. 1(a)]. The emitters are coupled to the waveguide with a decay rate $\Gamma = \beta\Gamma_{\rm tot}$ and radiate to the reservoir with the decay rate $\Gamma_{\rm tot}(1-\beta)$, where $\Gamma_{\rm tot}$ is the total decay rate of the emitters. Solving for the dynamics of this system can be approached in a variety of ways: it constitutes a cascaded quantum system [45,46] for which a master equation can be derived [31,34,46], but it is challenging to obtain general solutions as the number of emitters increases. Other approaches use a Green function to treat photon propagation, but generally require numerical solutions [47,48]. Here we develop an approach based on scattering matrices. We assume that the emitters are driven at a level well below saturation such that the dynamics of the system can be described by the one- and two-photon Fock states, and we thus compute the N-emitter scattering matrix for these manifolds. Computing the single-photon transmission is straightforward [49]. Significant research has been put into developing two-photon scattering matrices for a single emitter [50–55], and generalizations to N emitters have also been developed in the absence of loss [56–60]. Here we compute the N-emitter two-photon scattering matrix by projecting the input two-photon state on the scattering eigenstates, which can be determined using the Bethe ansatz technique as described in Ref. [52]. Computing the N-emitter scattering matrix then simply requires raising the eigenvalues to the Nth power.

The single frequency input coherent state is expressed up to the two-photon state as $|\alpha_{\rm in}\rangle = e^{-|\alpha|^2/2}[1+\alpha\hat{a}^\dagger_{k_0} + (\alpha^2/2)\hat{a}^\dagger_{k_0}\hat{a}^\dagger_{k_0}]|0\rangle$. We linearize and rescale the waveguide dispersion and set the group velocity $v_g = 1$, such that wave number and frequency, as well as distance and time, have the same units. Resonant photons correspond to $k_0 = 0$, and $\hat{a}^\dagger_{k_0}$ creates a photon with detuning k_0. Unlike bidirectional systems [61], in a chiral system the propagation phase between the emitters amounts to an overall phase in the Markovian limit and does not affect the dynamics [31,46]. The N-emitter scattering matrix for up to two photons is $\hat{S}^N = [\hat{S}_{11} + \hat{S}_{22} + \hat{S}_{12}]^N$. Here, $\hat{S}_{11}$ and $\hat{S}_{22}$ are the one- and two-photon scattering matrices, and $\hat{S}_{12}$ describes scattering of two input photons where one is transmitted and the other is lost. This term is required when $\beta < 1$. Note that to ensure that different decays add up incoherently, $\hat{S}_{12}$ contains the state of the photons which are lost. Using the orthogonality of the one- and two-photon subspaces, the scattering matrix restricted to one and two photons is

$$\hat{S}^N = \hat{S}^N_{11} + \hat{S}^N_{22} + \sum_{M=0}^{N-1} \hat{S}^{N-M-1}_{11}\hat{S}_{12}\hat{S}^M_{22}, \qquad (1)$$

and we define contributions to the output state as $\hat{S}^N|\alpha_{\rm in}\rangle \equiv |{\rm out}\rangle_1 + |{\rm out}\rangle_2 + |{\rm out}\rangle_{21}$. Here, we only consider the part of the scattering with outgoing photons. Computing $\hat{S}^N_{11}|\alpha_{\rm in}\rangle$ is simple: since the scattering matrix must conserve the photon energy, it simply multiplies the creation operator by a transmission coefficient: $a^\dagger_k \to t^N_k a^\dagger_k$ with $t_k = 1\text{–}2\beta/(1-2ik/\Gamma_{\rm tot})$ [54]. This is equivalent to scattering off a single-sided cavity. Consequently, the linear contribution to the output power scales exponentially with N, $\langle a^\dagger a\rangle_1 = |t_{k_0}|^{2N}|\alpha|^2/L$, where L is a quantization length. Thus, the linear single-photon response yields the usual exponential decay with N when $|t_{k_0}| < 1$.

Computing $\hat{S}^N_{22}|\alpha_{\rm in}\rangle$ is more involved. We do this by projecting the input state on the orthonormal set of two-photon scattering eigenstates computed in Ref. [52]. These consist of a set of extended states $|W_{E,\Delta}\rangle$, with position space representation $W_{E,\Delta}(x_c, x) = \sqrt{2}e^{iEx_c}[2\Delta\cos\Delta x - \Gamma{\rm sgn}(x)\sin\Delta x]/(2\pi\sqrt{4\Delta^2+\Gamma^2})$, where for two photon positions, x_1 and x_2, the center-of-mass and difference coordinates are $x_c = (x_1+x_2)/2$ and $x = x_1 - x_2$ [52]. The two indices of W are a two-photon detuning $E = k + p$ and a frequency difference of the two photons $\Delta = (k-p)/2$, where k and p are the detunings of the two photons. The remaining eigenstates are a set of bound states $|B_E\rangle$ with $B_E(x_c, x) = \sqrt{\Gamma/4\pi}e^{iEx_c}e^{-\Gamma/2|x|}$, which only vary with the two-photon detuning E.

The two-photon scattering matrix operating on the input state gives [52]

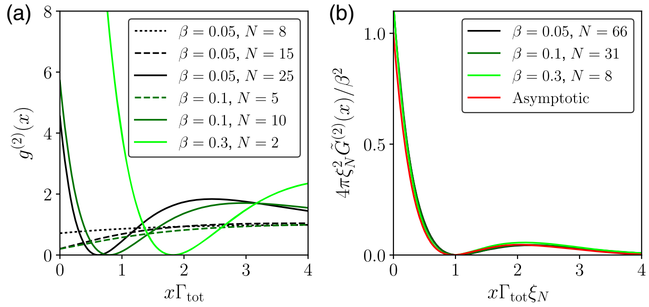

FIG. 2. (a) Normalized second-order correlation function $g^{(2)}(x)$ for different numbers of emitters N and coupling efficiencies β. As the optical depth increases, the correlation function becomes strongly bunched. (b) Second-order correlation function $\tilde{G}^{(2)}(x)$ scaled by $4\pi\xi_N^2/\beta^2$. The emitter numbers are chosen so that the linear transmission is $(1-2\beta)^{2N} \sim 10^{-6}$.

$$\frac{|\mathrm{out}\rangle_2}{A} = \tilde{t}_{2k_0}^N c_1 |B_{2k_0}\rangle - \int \frac{d\Delta t_{k_0+\Delta}^N t_{k_0-\Delta}^N}{\Delta\sqrt{1+4\frac{\Delta^2}{\Gamma^2}}} |W_{2k_0,\Delta}\rangle, \quad (2)$$

where, henceforth, integrals range over $\mathbb{R}$, $c_1 = \sqrt{8\pi/\Gamma}$, and $\tilde{t}_E = 1–4\beta/(1+\beta - iE/\Gamma_{\mathrm{tot}})$. Additionally, $A = \alpha^2/Le^{-|\alpha|^2/2} \sim P_{\mathrm{in}}$, where the input power is $P_{\mathrm{in}} = \alpha^2/L$, and we henceforth take α to be real. Using these eigenstates, we obtain a position representation of the full two-photon output state by performing the integration over Δ in Eq. (2). The special case of $\beta = 1$ has previously been treated and leads to a parity effect in the output state for a resonant drive [32,60]. The full two-photon output state is

$$|\mathrm{out}\rangle_2 = \frac{A}{2}\int dx_1 dx_2 \hat{a}^\dagger(x_1)\hat{a}^\dagger(x_2)|0\rangle\psi_N(x_c, x), \quad (3)$$

with $\psi_N(x_c, x) = e^{2ik_0x_c}[t_{k_0}^{2N} - \phi_N(x)]$. The $t_{k_0}^{2N}$ term corresponds to uncorrelated photons interacting individually with all N emitters while $\phi_N(x)$ contains the photon correlations induced by the interactions. We calculate the correlations $\phi_N(x)$ analytically, but for brevity, we leave the exact form to the Supplemental Material (SM) [62] and show only its asymptotic form below. The correlations induced by the photon-photon interactions are quantified by the normalized second-order correlations function $g^{(2)}(x) = \langle\hat{a}^\dagger(0)\hat{a}^\dagger(x)\hat{a}(x)\hat{a}(0)\rangle/\langle\hat{a}^\dagger\hat{a}\rangle = |\psi_N(x_c, x)|^2/|t_{k_0}|^{4N} + O(P_{\mathrm{in}}/P_{\mathrm{sat}})$, where the saturation power is $P_{\mathrm{sat}} = \Gamma_{\mathrm{tot}}/\beta$. Throughout the remainder of this Letter we consider a resonant drive $k_0 = 0$, as it generates the most interesting physics.

Figure 2(a) shows $g^{(2)}(x)$ for different β and N. As N increases, $g^{(2)}(x)$ becomes strongly bunched even for $\beta \ll 1$. This signifies that the output contains strong photon-photon correlations and happens because the linear component of the transmitted power $\sim|t_{k_0}|^{2N}$ decays exponentially with N while $\phi_N(x)$ does not. We can understand this by considering the Fourier transform of the correlated part of the two-photon wave packet $\phi_N(\Delta_k)$, where $\Delta_k = (k_1 - k_2)/2$, which we show in Fig. 3(a). Nonlinear interactions generate correlated frequency sidebands with $\Delta_k \neq 0$. Meanwhile, the loss of the system is strongest on resonance and, thus, frequency components $\Delta_k \sim 0$ suffer strong loss. This leads to a two-lobed shape in Fourier space whose inverse Fourier transform determines the shape of $g^{(2)}(x)$. The detuning of the peaks of $\phi_N(\Delta_k)$ increase with N, and thus loss due to each subsequent emitter decreases and the scaling of ϕ_N is subexponential. We highlight that this occurs for all $\beta < 1$ provided the optical depth is large. The slow decay of ϕ_N and the resulting large values $g^{(2)}(0)$ reveal that the transmission of the system is dominated by events where two simultaneously incident photons form a correlated state. For sufficiently large optical depth, photons interacting individually will be completely blocked and the transmission is therefore dominated by two-photon events leading to strong photon bunching.

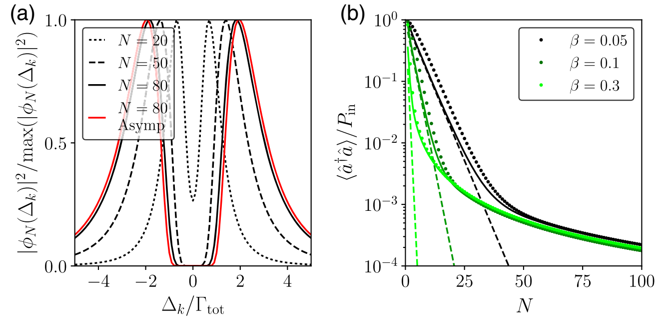

FIG. 3. (a) The normalized magnitude squared of the Fourier transform of the correlated part of the two-photon wave packet ϕ_N for $\beta = 0.05$ with the asymptotic expression plotted for $N = 80$ in red. (b) Normalized output intensity $\langle\hat{a}^\dagger\hat{a}\rangle/P_{\mathrm{in}}$ versus emitter number N. Broken lines show the linear output intensity $(1-2\beta)^{2N}$ for uncorrelated photon transport while the solid lines show the asymptotic scaling. For large optical depths the transmitted power shows a power-law decay $N^{-3/2}$. The input power is $P_{\mathrm{in}} = 0.1P_{\mathrm{sat}}$.

We now derive an asymptotic expression for the nonexponentially decaying parts of ϕ_N. Since detuned Fourier components dominate, we expand the second term in Eq. (2) to second order in $\Gamma_{\mathrm{tot}}/\Delta$ and get $t_\Delta^N t_{-\Delta}^N \sim \exp(-\Gamma_{\mathrm{tot}}^2\xi_N^2/\Delta^2)$, where $\xi_N = \sqrt{N\beta(1-\beta)}$. This gives us a compact expression for the output state in Fourier space (see SM [62]):

$$|\mathrm{out}\rangle_2 \sim -\frac{A\Gamma}{2}\int dk\hat{a}^\dagger(k)\hat{a}^\dagger(-k)|0\rangle\frac{e^{-\xi_N^2\Gamma_{\mathrm{tot}}^2/k^2}}{k^2}. \quad (4)$$

The detuned Fourier components thus dominate when $\xi_N^2 \gg 1$. The functional form of this result determines the shape of the curves in Fig. 3(a) and its inverse

Fourier transform gives the shape of $g^{(2)}(x)$ shown in Fig. 2(b). Importantly, it also reveals that the dynamics of two-photon transport is governed universally by ξ_N. This is closely related to the optical depth for a resonant drive, which is $\log[(1-2\beta)^{2N}] \sim 4\xi_N^2$ when $\beta \sim 0$ or $\beta \sim 1$. We highlight this in Fig. 2(b), which shows the correlation function $\tilde{G}^{(2)}(x) = \langle \hat{a}^\dagger(0)\hat{a}^\dagger(x)\hat{a}(x)\hat{a}(0)\rangle / P_{\mathrm{in}}^2$. This is given by

$$\tilde{G}^{(2)}(x) \sim \frac{\beta^2}{4\pi^2\xi_N^2}[\tilde{G}(\xi_N \Gamma_{\mathrm{tot}} x)]^2, \tag{5}$$

where $\tilde{G}(x) = \int dk \cos(kx) e^{-1/k^2}/k^2$. The correlation function $\tilde{G}^{(2)}(x)$ then has the same form for all values of β and N as long as the optical depth is large. The value $\tilde{G}^{(2)}(0) = \beta^2/4\pi\xi_N^2$ and the width of $\tilde{G}^{(2)}(x)$ scales $\propto 1/\sqrt{N}$. The correlations arising from the complex interplay between nonlinear photon interactions and dissipation can therefore be expressed in a compact universal form with a simple scaling parameter.

We now turn to the output power. This requires us to compute the contribution due to the last term in Eq. (1). Here we construct $\hat{S}_{12}$ by transforming from our picture of a chiral scattering process to one that contains transmission and reflection, where the coupling to the backward mode is given by our decay rate to the loss reservoir $\Gamma_{\mathrm{tot}}(1-\beta)$. In this picture we simply compute the scattering amplitude for one photon transmitted and one reflected. This is done by adapting standard two-photon scattering matrices for a single emitter (see SM [62]) [54]. We do this independently for each emitter such that there are no collective effects through the loss reservoir, which is a good approximation for randomly positioned nonsubwavelength emitter separations [63]. Using this scattering matrix we obtain a state which can be compactly written as

$$|\mathrm{out}\rangle_{21} = \frac{A}{2}\sum_{M=0}^{N-1}\int dk \hat{a}_R^\dagger(k)\hat{a}_L^{\dagger(M+1)}(k)|0\rangle t_k^{N-M-1} b_M(k), \tag{6}$$

where $\hat{a}_R^\dagger(k)$ and $\hat{a}_L^{\dagger(M+1)}(k)$ create right- and left-going photons and the superscript $M+1$ ensures there are no collective effects. The function $b_M(k_1)$ depends on ψ_M, and for brevity we leave its exact form for the SM [62]. Importantly, with the state $|\mathrm{out}\rangle_{21}$ at hand we can compute the power $\langle \hat{a}^\dagger \hat{a}\rangle$. Using our exact expressions for $\psi_N(x_c, x)$ and $b_M(k)$, we obtain an expression for $\langle \hat{a}^\dagger \hat{a}\rangle$ containing integrals which we evaluate numerically. These results are shown in Fig. 3(b) for different β and N. Here, uncorrelated photon transport suffers exponential decay with N. Interestingly, we observe that the transmitted power deviates from exponential decay and for large N follows a power law. The nonlinear power transmission therefore dominates for large optical depths.

We use Eqs. (4) and (6) to compute a simple asymptotic expression for the transmitted power (see SM for details [62]),

$$\frac{\langle \hat{a}^\dagger \hat{a}\rangle}{P_{\mathrm{in}}} \sim (1-2\beta)^{2N} + \frac{P_{\mathrm{in}}}{P_{\mathrm{sat}}}\frac{\beta}{4\sqrt{\pi}\xi_N^3}\frac{3-2\beta(1-\beta)}{1-2\beta(1-\beta)}, \tag{7}$$

implying a nonlinear power scaling of $1/N^{3/2}$. Figure 3(b) shows excellent agreement between the full calculation and the asymptotic scaling. Finally, we note that the nonlinear power has contributions from $\hat{S}_{22}$ and $\hat{S}_{12}$, i.e., photon pairs and single photons; the nonlinear power contribution of pairs relative to single photons is $\langle \hat{a}^\dagger \hat{a}\rangle_2 / \langle \hat{a}^\dagger \hat{a}\rangle_{21} \sim 1/\{2\sqrt{2} - 1 + 4\sqrt{2}/[1-2\beta(1-\beta)]\}$ (see SM [62]), which is largest for $\beta \sim 0$ and $\beta \sim 1$ giving ~ 0.13, and smallest for $\beta = 1/2$ giving ~ 0.08.

The physics presented here can be observed experimentally by measuring $g^{(2)}$ and $\langle \hat{a}^\dagger \hat{a}\rangle$ of the transmitted light. The nonlinear scaling of the output power and strong photon bunching are clear signals of nonlinear dynamics. State-of-the-art experimental systems that exhibit chiral light-matter interaction include quantum dots and atoms coupled to photonic nanostructures [27,28,64]. In quantum dot systems the emission can be close to unidirectional and $\beta \sim 1$ [28,64–66]; however, it is difficult to tune several quantum dots into resonance. On the other hand, hundreds of atoms can be trapped in the evanescent field of a nanofiber and exhibit chiral light-matter interaction [27,39–42], albeit with $\beta \ll 1$. These have a directionality of $\sim 90\%$ and thus couple residually to the backward propagating mode, which has not been taken into account in the analytics here.

We numerically model a system with parameters similar to a nanofiber with coupling to the forward propagating mode $\beta = 0.05$ and coupling to the backward mode $\beta_L = 0.005$, where the total emission rate to the waveguide is $\Gamma_{\mathrm{tot}}(\beta + \beta_L)$. We additionally model a fully bidirectional system with $\beta_L = \beta$. We use a wave function formalism where we restrict to two excitations in the system [67,68], and consider $N = 20, 30, 50, 100$ emitters. The emitters are positioned randomly such that backscattering does not add up coherently. For each parameter set we consider 100 realizations. Figure 4(a) shows the mean $\langle g^{(2)}(x)\rangle$ for $N = 30$ when considering the ensemble. The mean agrees quantitatively with the exact unidirectional theory, while the standard deviation for $\beta_L = \beta$ shows minor discrepancies near $x \sim 0$ with standard deviation $\Delta g_{1:1}^{(2)}(0) = 15$. For $\beta_L = 0.005$, the standard deviation is negligible and is not shown. The asymptotic theory has a slight discrepancy because the parameters do not fall in this limit since $\xi_N^2 = 1.425$. Figure 4(b) shows the mean output power, which is also in excellent agreement with the unidirectional theory. The standard deviation of the power is insignificant on this scale and is not shown. The effects of backscattering can thus be ignored provided the number

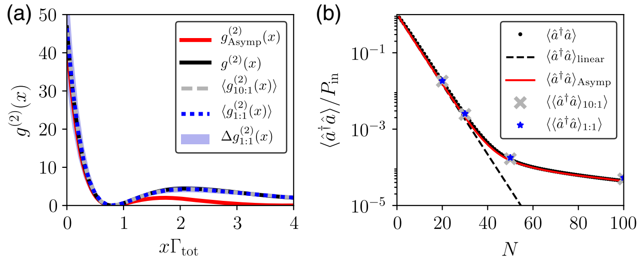

FIG. 4. (a) Normalized second-order correlation function for $\beta = 0.05$ and $N = 30$. Curves show asymptotic theory $g^{(2)}_{\mathrm{Asymp}}(x)$, exact theory $g^{(2)}(x)$, and mean of numerical simulation with $\beta_L = 0.005$ and $\beta_L = 0.05$, $\langle g^{(2)}_{10:1}(x) \rangle$ and $\langle g^{(2)}_{1:1}(x) \rangle$, respectively. All curves, but the asymptotic theory, lie on top of one another. Shading shows the standard deviation $\Delta g^{(2)}_{1:1}(x)$ for $\beta_L = \beta$. (b) Normalized output power versus emitter number for $\beta = 0.05$ and $P_{\mathrm{in}}/P_{\mathrm{sat}} = 0.02$ showing the analytic theory $\langle \hat{a}^\dagger \hat{a} \rangle$, asymptotic theory $\langle \hat{a}^\dagger \hat{a} \rangle_{\mathrm{Asymp}}$, and exponential damping $\langle \hat{a}^\dagger \hat{a} \rangle_{\mathrm{linear}}$. Mean of the numerical results with $\beta_L = \beta/10$ and $\beta_L = \beta$ are $\langle \langle \hat{a}^\dagger \hat{a} \rangle_{10:1} \rangle$ and $\langle \langle \hat{a}^\dagger \hat{a} \rangle_{1:1} \rangle$, respectively.

of emitters is sufficiently large and the emitters are positioned randomly.

In order to observe the physics here, P_{in} and N should be chosen such that the optical depth is sufficiently large, while the output power should be sufficiently bright to measure experimentally. We find that for $\beta = 0.05$ and $N = 30$, one ideally expects a value of $g^{(2)}(0) = 47$. If we consider an optical transition with $\Gamma_{\mathrm{tot}} = 2\pi \times 5$ MHz driven with $P_{\mathrm{in}}/P_{\mathrm{sat}} = 0.05$, we compute an output power of $\langle \hat{a}^\dagger \hat{a} \rangle = 105$ kHz, with the linear part of the power being 1.2 times larger than the nonlinear part. We also compute a coincidence rate of 1.7 kHz, where we define a coincidence as two photons separated by less than $3/\Gamma_{\mathrm{tot}}$. These outputs are sufficiently bright for detection by single-photon detectors. Including the nonlinear power contribution to estimate the second-order correlation for this input power gives $g^{(2)}(0) \sim 25$. This result can be rescaled for other β and N using Eqs. (5) and (7).

In conclusion, we have analyzed the dynamics of photon-photon interactions mediated by an optically deep ensemble of emitters coupled to a waveguide. The system exhibits rich out-of-equilibrium physics due to a combination of highly nonlinear driven systems and dissipation. The emitter-induced photon-photon correlation reveals itself through the formation of bunched states of light and a universal power-law scaling of the transmission for large optical depths. As a consequence, for a sufficiently large optical depth the transmission becomes completely dominated by correlated photons. Remarkably, the formation of the strongly correlated photon states happens even for emitters weakly coupled to a waveguide and can thus be directly observed, e.g., with atoms near optical nanofibers. The present results thus open up a new avenue for studying such phenomena.

S. M. and K. H. acknowledge support through DFG (GRK 1991). A. S. S. and S. D. acknowledge financial support from the European Union Seventh Framework Programme through the ERC Grant QIOS (Grant No. 306576) and the Danish council for independent research (Natural Sciences). P. L. gratefully acknowledges financial support from the European Research Council (ERC Advanced Grant "SCALE"). P. L. and A. S. S. gratefully acknowledge financial support from the Danish National Research Foundation (Center of Excellence "Hy-Q").

*sahand.mahmoodian@itp.uni-hannover.de

[1] A. Polkovnikov, K. Sengupta, A. Silva, and M. Vengalattore, Rev. Mod. Phys. **83**, 863 (2011).
[2] J. Eisert, M. Friesdorf, and C. Gogolin, Nat. Phys. **11**, 124 (2015).
[3] J. I. Cirac and P. Zoller, Nat. Phys. **8**, 264 (2012).
[4] S. Datta, *Electronic Transport in Mesoscopic Systems* (Cambridge University Press, Cambridge, England, 1997).
[5] S. Das Sarma, S. Adam, E. H. Hwang, and E. Rossi, Rev. Mod. Phys. **83**, 407 (2011).
[6] E. A. Laird, F. Kuemmeth, G. A. Steele, K. Grove-Rasmussen, J. Nygård, K. Flensberg, and L. P. Kouwenhoven, Rev. Mod. Phys. **87**, 703 (2015).
[7] D. E. Chang, A. S. Sørensen, E. A. Demler, and M. D. Lukin, Nat. Phys. **3**, 807 (2007).
[8] I. Carusotto and C. Ciuti, Rev. Mod. Phys. **85**, 299 (2013).
[9] D. E. Chang, V. Vuletić, and M. D. Lukin, Nat. Photonics **8**, 685 (2014).
[10] Y. O. Dudin and A. Kuzmich, Science **336**, 887 (2012).
[11] V. Parigi, E. Bimbard, J. Stanojevic, A. J. Hilliard, F. Nogrette, R. Tualle-Brouri, A. Ourjoumtsev, and P. Grangier, Phys. Rev. Lett. **109**, 233602 (2012).
[12] T. Peyronel, O. Firstenberg, Q.-Y. Liang, S. Hofferberth, A. V. Gorshkov, T. Pohl, M. D. Lukin, and V. Vuletić, Nature (London) **488**, 57 (2012).
[13] D. Maxwell, D. J. Szwer, D. Paredes-Barato, H. Busche, J. D. Pritchard, A. Gauguet, K. J. Weatherill, M. P. A. Jones, and C. S. Adams, Phys. Rev. Lett. **110**, 103001 (2013).
[14] S. Baur, D. Tiarks, G. Rempe, and S. Dürr, Phys. Rev. Lett. **112**, 073901 (2014).
[15] J. D. Thompson, T. L. Nicholson, Q.-Y. Liang, S. H. Cantu, A. V. Venkatramani, S. Choi, I. A. Fedorov, D. Viscor, T. Pohl, M. D. Lukin, and V. Vuletić, Nature (London) **542**, 206 (2017).
[16] M. F. Maghrebi, M. J. Gullans, P. Bienias, S. Choi, I. Martin, O. Firstenberg, M. D. Lukin, H. P. Büchler, and A. V. Gorshkov, Phys. Rev. Lett. **115**, 123601 (2015).
[17] O. Firstenberg, T. Peyronel, Q.-Y. Liang, A. V. Gorshkov, M. D. Lukin, and V. Vuletić, Nature (London) **502**, 71 (2013).
[18] M. J. Gullans, J. D. Thompson, Y. Wang, Q.-Y. Liang, V. Vuletić, M. D. Lukin, and A. V. Gorshkov, Phys. Rev. Lett. **117**, 113601 (2016).
[19] K. Jachymski, P. Bienias, and H. P. Büchler, Phys. Rev. Lett. **117**, 053601 (2016).
[20] Q.-Y. Liang, A. V. Venkatramani, S. H. Cantu, T. L. Nicholson, M. J. Gullans, A. V. Gorshkov, J. D. Thompson,

C. Chin, M. D. Lukin, and V. Vuletić, Science **359**, 783 (2018).

[21] A. Goban, C.-L. Hung, S.-P. Yu, J. D. Hood, J. A. Muniz, J. H. Lee, M. J. Martin, A. C. McClung, K. S. Choi, D. E. Chang, O. Painter, and H. J. Kimble, Nat. Commun. **5**, 3808 (2014).

[22] T. G. Tiecke, J. D. Thompson, N. P. de Leon, L. R. Liu, V. Vuletić, and M. D. Lukin, Nature (London) **508**, 241 (2014).

[23] B. Hacker, S. Welte, G. Rempe, and S. Ritter, Nature (London) **536**, 193 (2016).

[24] M. Arcari, I. Söllner, A. Javadi, S. Lindskov Hansen, S. Mahmoodian, J. Liu, H. Thyrrestrup, E. H. Lee, J. D. Song, S. Stobbe, and P. Lodahl, Phys. Rev. Lett. **113**, 093603 (2014).

[25] P. Lodahl, S. Mahmoodian, and S. Stobbe, Rev. Mod. Phys. **87**, 347 (2015).

[26] J. Petersen, J. Volz, and A. Rauschenbeutel, Science **346**, 67 (2014).

[27] R. Mitsch, C. Sayrin, B. Albrecht, P. Schneeweiss, and A. Rauschenbeutel, Nat. Commun. **5**, 5713 (2014).

[28] I. Söllner, S. Mahmoodian, S. L. Hansen, L. Midolo, G. Kirsanske, T. Pregnolato, H. El-Ella, E. H. Lee, J. D. Song, S. Stobbe, and P. Lodahl, Nat. Nanotechnol. **10**, 775 (2015).

[29] A. B. Young, A. C. T. Thijssen, D. M. Beggs, P. Androvitsaneas, L. Kuipers, J. G. Rarity, S. Hughes, and R. Oulton, Phys. Rev. Lett. **115**, 153901 (2015).

[30] R. J. Coles, D. M. Price, J. E. Dixon, B. Royall, E. Clarke, P. Kok, M. S. Skolnick, A. M. Fox, and M. N. Makhonin, Nat. Commun. **7**, 11183 (2016).

[31] P. Lodahl, S. Mahmoodian, S. Stobbe, A. Rauschenbeutel, P. Schneeweiss, J. Volz, H. Pichler, and P. Zoller, Nature (London) **541**, 473 (2017).

[32] K. Stannigel, P. Rabl, and P. Zoller, New J. Phys. **14**, 063014 (2012).

[33] T. Ramos, H. Pichler, A. J. Daley, and P. Zoller, Phys. Rev. Lett. **113**, 237203 (2014).

[34] H. Pichler, T. Ramos, A. J. Daley, and P. Zoller, Phys. Rev. A **91**, 042116 (2015).

[35] S. Mahmoodian, P. Lodahl, and A. S. Sørensen, Phys. Rev. Lett. **117**, 240501 (2016).

[36] M. Scheucher, A. Hilico, E. Will, J. Volz, and A. Rauschenbeutel, Science **354**, 1577 (2016).

[37] E. Zeuthen, M. J. Gullans, M. F. Maghrebi, and A. V. Gorshkov, Phys. Rev. Lett. **119**, 043602 (2017).

[38] C. R. Murray, I. Mirgorodskiy, C. Tresp, C. Braun, A. Paris-Mandoki, A. V. Gorshkov, S. Hofferberth, and T. Pohl, Phys. Rev. Lett. **120**, 113601 (2018).

[39] C. Sayrin, C. Junge, R. Mitsch, B. Albrecht, D. O'Shea, P. Schneeweiss, J. Volz, and A. Rauschenbeutel, Phys. Rev. X **5**, 041036 (2015).

[40] H. L. Sørensen, J.-B. Béguin, K. W. Kluge, I. Iakoupov, A. S. Sørensen, J. H. Müller, E. S. Polzik, and J. Appel, Phys. Rev. Lett. **117**, 133604 (2016).

[41] N. V. Corzo, B. Gouraud, A. Chandra, A. Goban, A. S. Sheremet, D. V. Kupriyanov, and J. Laurat, Phys. Rev. Lett. **117**, 133603 (2016).

[42] P. Solano, J. A. Grover, J. E. Hoffman, S. Ravets, F. K. Fatemi, L. A. Orozco, and S. L. Rolston, *Advances In Atomic, Molecular, and Optical Physics* (Elsevier, New York, 2017), Vol. 66, pp. 439–505.

[43] H. E. Stanley, *Phase Transitions and Critical Phenomena* (Clarendon Press, Oxford, 1971).

[44] J. M. T. Thompson and H. B. Stewart, *Nonlinear Dynamics and Chaos* (John Wiley & Sons, New York, 2002).

[45] H. J. Carmichael, Phys. Rev. Lett. **70**, 2273 (1993).

[46] C. W. Gardiner, Phys. Rev. Lett. **70**, 2269 (1993).

[47] A. Asenjo-Garcia, J. D. Hood, D. E. Chang, and H. J. Kimble, Phys. Rev. A **95**, 033818 (2017).

[48] M. T. Manzoni, D. E. Chang, and J. S. Douglas, Nat. Commun. **8**, 1743 (2017).

[49] J. T. Shen and S. Fan, Opt. Lett. **30**, 2001 (2005).

[50] K. Kojima, H. F. Hofmann, S. Takeuchi, and K. Sasaki, Phys. Rev. A **68**, 013803 (2003).

[51] H. F. Hofmann, K. Kojima, S. Takeuchi, and K. Sasaki, Phys. Rev. A **68**, 043813 (2003).

[52] J.-T. Shen and S. Fan, Phys. Rev. A **76**, 062709 (2007).

[53] H. Zheng, D. J. Gauthier, and H. U. Baranger, Phys. Rev. A **82**, 063816 (2010).

[54] S. Fan, Ş. E. Kocabaş, and J.-T. Shen, Phys. Rev. A **82**, 063821 (2010).

[55] T. Shi, D. E. Chang, and J. I. Cirac, Phys. Rev. A **92**, 053834 (2015).

[56] V. I. Rupasov, JETP Lett. **36**, 142 (1982).

[57] V. I. Rupasov and V. I. Yudson, Sov. Phys. JETP **59**, 478 (1984).

[58] V. I. Yudson, Sov. Phys. JETP **88**, 1043 (1985).

[59] M. Pletyukhov and V. Gritsev, New J. Phys. **14**, 095028 (2012).

[60] M. Ringel, M. Pletyukhov, and V. Gritsev, New J. Phys. **16**, 113030 (2014).

[61] D. E. Chang, L. Jiang, A. V. Gorshkov, and H. J. Kimble, New J. Phys. **14**, 063003 (2012).

[62] See Supplemental Material at http://link.aps.org/supplemental/10.1103/PhysRevLett.121.143601 for contains details of calculations presented in the main text.

[63] A. Asenjo-Garcia, M. Moreno-Cardoner, A. Albrecht, H. J. Kimble, and D. E. Chang, Phys. Rev. X **7**, 031024 (2017).

[64] A. Javadi, D. Ding, M. H. Appel, S. Mahmoodian, M. C. Löbl, I. Söllner, R. Schott, C. Papon, T. Pregnolato, S. Stobbe, L. Midolo, T. Schröder, A. D. Wieck, A. Ludwig, R. J. Warburton, and P. Lodahl, Nat. Nanotechnol. **13**, 398 (2018).

[65] S. Mahmoodian, K. Prindal-Nielsen, I. Söllner, S. Stobbe, and P. Lodahl, Opt. Mater. Express **7**, 43 (2017).

[66] D. L. Hurst, D. M. Price, C. Bentham, M. N. Makhonin, B. Royall, E. Clarke, P. Kok, L. R. Wilson, M. S. Skolnick, and A. M. Fox, Nano Lett. **18**, 5475 (2018).

[67] M. Čepulkovskis, Nonlinear photon interactions in waveguides, Master's thesis, University of Copenhagen, 2017.

[68] S. Das (to be published).